SAND2018-11325C

ERROR FIELD IMPACT ON MODE LOCKING AND DIVERTOR HEAT FLUX IN NSTX-U

N.M. Ferraro, J.-K. Park, A. Brooks, S.P. Gerhardt, J. Menard
Princeton Plasma Physics Laboratory
Princeton, NJ United States
Email: nferraro@pppl.gov

C.E. Myers
Sandia National Laboratories
Albuquerque, NM United States

S. Munaretto
General Atomics
San Diego, CA United States

M.L. Reinke
Oak Ridge National Laboratory
Oak Ridge, TN United States

Abstract

Results from the 2016 NSTX-U campaign and the subsequent recovery effort have led to new insights regarding error fields in the NSTX-U experiment in particular, and in spherical tokamak configurations in general. During the experimental campaign, many L-mode discharges were found to be locked from the $q = 2$ surface outward, indicating the presence of error fields. Extensive metrology and plasma response modeling with IPEC and M3D-C1 indicate that misalignment of the toroidal field coil (TF) center rod, while small, produces the largest resonant error field among the sources considered. The plasma response to the TF error field is shown to depend significantly on the presence of a $q = 1$ surface, in qualitative agreement with experimental observations. It is found that certain characteristics of the TF error field present new challenges for error field correction. Specifically, the error field spectrum differs significantly from that of coils on the low-field side (such as the NSTX-U RMP coils), and does not resonate strongly with the dominant kink mode, thus potentially requiring a multi-mode correction. Finally, to mitigate heat fluxes using poloidal flux expansion, the pitch angle at the divertor plates must be small (~1°). It is shown that uncorrected error fields may result in potentially significant local perturbation to the pitch angle. Tolerances for coil alignments in the NSTX-U restart are derived based on both heat flux considerations and core resonant fields independently.

1. INTRODUCTION

Error fields—non-axisymmetric magnetic fields present in tokamaks due to misaligned magnets or currents in external conducting structures—are well known to have deleterious effects on plasma performance. These effects can include mode locking [1], rotation braking from neoclassical toroidal viscosity (NTV) [2], and a reduction in thermal particle confinement ("pump out") [3, 4]. Much work has been done on characterizing error fields on various tokamaks, and on correcting these error fields either using trim coils [5, 6] or by reducing errors in coil positioning and shape [7]. Fortunately, it is found that the plasma is often most sensitive to a particular error field distribution, with much lower sensitivity to orthogonal distributions, in which case error field correction (EFC) can be effective with just a single trim coil set [8]. Models assuming that the plasma response is entirely due to a single error field distribution are known as "single-mode" models, and are presently used successfully for EFC [9].

Observations from NSTX-U [10] operations in 2016 reveal the signatures of significant error fields. In particular, it is found that many L-mode discharges were locked from the $q = 2$ surface outward. There is no evidence of a distinct locking event, and it is believed that the plasma edge was locked *ab initio*. Error field correction using the NSTX-U mid-plane RMP coils is unsuccessful in preventing or unlocking the edge before causing the core also to lock, leading to disruption. This demonstrates the presence of multiple modes to which the plasma is sensitive.

EFC in NSTX-U is impeded not only by the influence of multiple modes, but by a dramatic change in optimal EFC phase over the duration of a discharge. Figure 1 shows the results of a scan of early-time error field correction (EFC) in 1 MW L-mode discharges in NSTX-U. In each case, a square EFC waveform of 600 A (1.2 kA-turns) is applied shortly after t = 0 at various phases. Using the core rotation as a proxy for the efficacy of a

particular EFC phase, we infer that the optimum phase changes from $\varphi = 200^\circ$ early in time to $\varphi = 80^\circ$ in the flattop. This phase rotation constitutes a time (and/or scenario) dependent error field that would require a sophisticated EFC algorithm to correct. We note that the time of the phase change (roughly $t = 400$ ms) is nearly coincident with the formation of the q = 1 surface, which implies a significant $m/n = 1$ component of the error field. We show later that this is consistent with the error from a misaligned TF center rod.

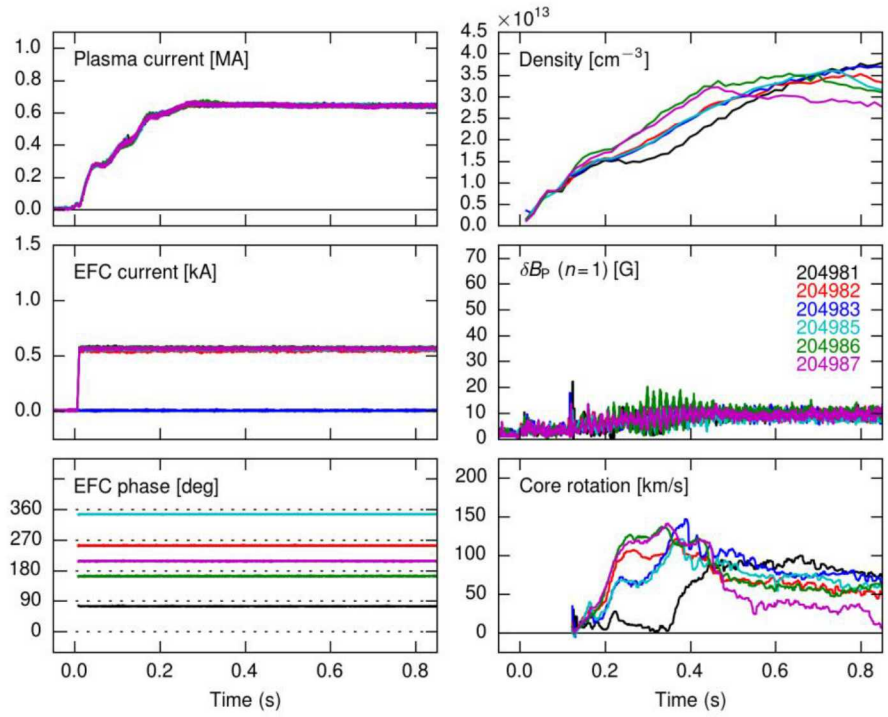

FIG 1. Scan of early-time externally applied error field correction (EFC) phase in 1 MW L-mode discharges in NSTX-U. The amplitude of the EFC is 1.2 kA-turns in all cases, while the phase is varied from shot to shot. In the panel showing core rotation at the bottom right, a phase dependence of the plasma response is clearly visible.

Given the inability to correct the error fields with the existing trim coils, significant effort has been made to understand the sources of error fields in NSTX-U as constructed in 2016, and to ensure that error fields are reduced to a more manageable level when NSTX-U resumes operation. This effort has involved extensive metrology, summarized in section 2.1, and plasma response calculations, described in section 3. Criteria for limiting the potential consequences of the error fields both on core braking and heat flux to the divertor plates are used to inform the physics basis for tolerances in NSTX-U.

2. CHARACTERIZATION OF ERROR FIELDS IN NSTX-U

2.1. Metrology

At the conclusion of the 2016 NSTX-U campaign, extensive metrology was conducted on the primary vertical field ("PF5") coils, and the center stack assembly, which includes the central solenoid and the center rod of the toroidal field ("TF") coils. The relative positions of the inner face of the vessel wall and the center stack casing was measured using a ROMER Arm. Combining these measurements with ruler-based measurements of the distance between the PF5 and the outer vessel wall yields the PF5 radius as a function of toroidal angle. The n = 1–3 Fourier components of these measurements, shown in table 1, reveal shifts (n = 1 component) of roughly 5 mm of the PF5U and PF5L coils relative to the vertical axis of the ROMER Arm coordinate system, as well as significant non-circularities. Unlike the vacuum vessel, the PF5 coil shapes differ from measurements made in 2004. This is most likely due to the fact that the radial restraints on the PF5 coils [7] were reconfigured during the upgrade to provide more freedom for the thermal expansion that is expected when operating at full NSTX-U parameters. The shift and tilt of the TF center rod were determined by combining the ROMER Arm data with data additional metrology conducted after the center-stack assembly was removed from the machine using a FARO Laser Tracker. The Laser Tracker was used to measure the relative positions of the inboard vertical divertor targets (IBDV) and the faces of the flags on the TF center rod. The resulting position of the upper and

lower TF flag faces in ROMER Arm coordinates defines the absolute shift and tilt of the TF center rod, shown in table 2.

TABLE 1. FOURIER COMPONENTS OF MEASURED HORIZONTAL DEVIATION OF PF5 COILS

Coil	$\delta R_{n=1}$	$\varphi_{n=1}$	$\delta R_{n=2}$	$\varphi_{n=2}$	$\delta R_{n=3}$	$\varphi_{n=3}$
PF5U	4.09 mm	121°	3.42 mm	113°	4.01 mm	323°
PF5L	6.19 mm	55°	4.09 mm	11°	9.45 mm	292°

TABLE 2. MEASURED SHIFT AND TILT OF CS CASING AND TF CENTER ROD

	Shift	Shift Angle	Tilt	Tilt Angle
CS Casing	1.8 mm	242°	0.15 mrad	156°
TF Center Rod	4.9 mm	246°	1.15 mrad	206°

2.2. Error Field Spectrum

The misalignments of the TF and PF coils result in an error field. For small shifts and tilts of the coils, the resulting error field will be linear in the shift and tilt and have toroidal mode number $n = 1$. In general, for a coil that produces field $\mathbf{B}^c$ in a coordinate system (r, ϕ, z) in which the coil is axisymmetric, the $n = 1$ component of that field in a coordinate system (R, φ, Z) such that (r, ϕ, z) is shifted by distance δ in direction φ_s and rotated through an angle α about axis φ_t relative to (R, φ, Z) is

$$\delta\mathbf{B} = \delta\, e^{i(\varphi-\varphi_s)}\left\{\left[-\partial_r B_r^c + i\frac{1}{R}B_\phi^c\right]\hat{\mathbf{R}} - \left[i\frac{1}{R}B_r^c + \partial_r B_\phi^c\right]\hat{\boldsymbol{\varphi}} - \partial_r B_z^c\,\hat{\mathbf{Z}}\right\}$$
$$+\,\alpha\, e^{i(\varphi-\varphi_t)}\begin{Bmatrix}\left[i(R\,\partial_z B_r^c - Z\,\partial_r B_r^c) - \frac{Z}{R}B_\phi^c + i\,B_z^c\right]\hat{\mathbf{R}} \\ +\left[i(R\,\partial_z B_\phi^c - Z\,\partial_r B_\phi^c) + \frac{Z}{R}B_r^c - B_z^c\right]\hat{\boldsymbol{\varphi}} \\ +\left[i(R\,\partial_z B_z^c - Z\,\partial_r B_z^c) + B_\phi^c - i\,B_r^c\right]\hat{\mathbf{Z}}\end{Bmatrix}$$

to lowest order in δ and α. This is consistent with the result La Haye and Scoville obtained for shifts and tilts of poloidal field coils [11]. We note here that this error field can be written as an ideal MHD displacement $\delta\mathbf{B} = \nabla\times(\boldsymbol{\xi}\times\mathbf{B})$ where

$$\boldsymbol{\xi} = \delta\, e^{i(\varphi-\varphi_s)}\left(\hat{\mathbf{R}} + i\,\hat{\mathbf{Z}}\right) + \alpha\, e^{i(\varphi-\varphi_t)}\left(i\,Z\,\hat{\mathbf{R}} - Z\,\hat{\boldsymbol{\varphi}} - i\,R\,\hat{\mathbf{Z}}\right)$$

To understand the effect of the error field on the plasma, it is convenient to consider the Fourier components of the normal component of the error field in straight field-line magnetic coordinates (ψ, θ, φ) based on the magnetic equilibrium in the absence of coil misalignments:

$$\delta B_{mn}(\psi) = \frac{1}{(2\pi)^2 S}\oiint d\theta\, d\varphi\; \Im\, \delta B\cdot\nabla\psi\, e^{i\,m\,\theta - i\,n\,\varphi}$$

Here S is the surface area of the magnetic surface labeled by ψ; θ and φ are the poloidal and toroidal angles, respectively, and $\Im = (\nabla\psi\cdot\nabla\theta\times\nabla\varphi)^{-1}$. We note that the error field spectrum depends on the coordinate system in which the field is measured. However, when the perturbed equilibrium is calculated, this calculation, if properly done, should account for any resultant shift or tilt of the magnetic axis of the plasma. Therefore, while the spectral components are coordinate-dependent, physical attributes of the perturbed equilibrium such as the width of magnetic islands will be coordinate-independent.

Here, we consider the error fields generated by shifting or tilting coils with respect to the the ROMER Arm coordinates, which we take to be the frame of the initial plasma equilibrium, or "lab" frame. These error fields depend linearly on the current in the misaligned coil, and are therefore scenario-dependent. The spectral decomposition also depends on the chosen axisymmetric equilibrium. Therefore we have considered a number

of NSTX-U scenarios as part of this study, including reconstructions of L-mode discharge 204077 at times t = 307 ms and t = 697 ms (which are before and after the formation of the q = 1 surface, respectively); and several 1.5 MA and 2 MA H-mode model scenarios based on scaled profiles from NSTX discharges.

The error field spectrum (ignoring the plasma response) is relatively insensitive to the plasma shape, especially in the plasma core. The spectrum calculated for NSTX-U discharge 204077 at t = 697 ms is shown in figure 2. The primary differences in error fields among scenarios is the magnitude of the error field (due to differing coil currents) and the locations of the mode-rational surfaces.

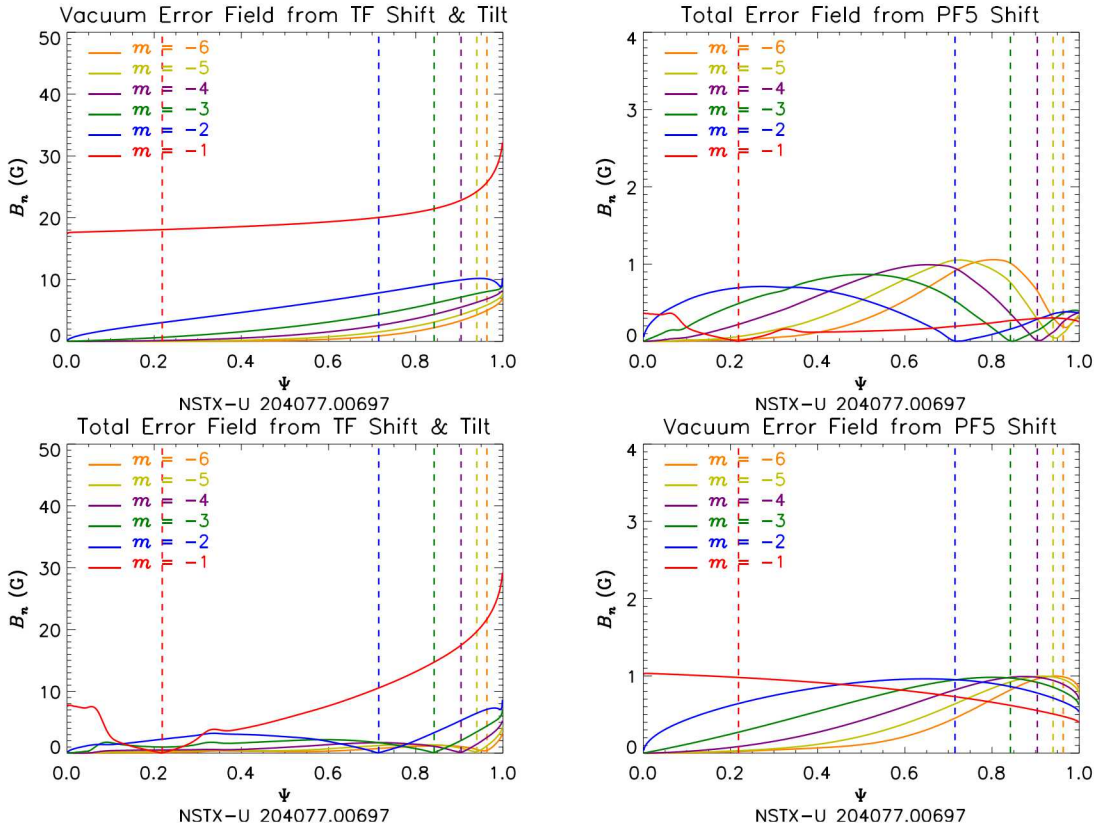

FIG 2. Top*: the n = 1, |m| = 1–6 spectral components of the error field due to the PF5 (*left*) and TF (*right*) coils as calculated by M3D-C1 in NSTX-U discharge 204077 at t = 697.* Bottom*: the total field (error field plus plasma response) in the perturbed equilibria for the same two cases.*

3. ANALYSIS OF THE IMPACT OF ERROR FIELDS

3.1. Braking and Locking

Resonant braking is estimated by calculating the 2/1 total resonant field in the perturbed equilibrium. Perturbed equilibrium calculations using both IPEC [12] and M3D-C1 [13, 14] find that the TF error field is the dominant source of resonant braking, despite the fact that the TF error field spectrum couples relatively weakly to the plasma, due to the large current in the TF rod and the proximity of the rod to the plasma. The plasma response to the TF error field is found to depend significantly on the presence of a q = 1 surface, since the TF error field is dominantly m/n = 1/1. This is qualitatively consistent with results of several "compass" scans performed during the NSTX-U run campaign, which found that the optimal error field correction before and after the formation of the q = 1 surface differed significantly. Interestingly, these discharges typically disrupted via locking of the 1/1 surface, since the 2/1 surface was often locked *ab initio*. The 1/1 component of the RMP coil spectrum is relatively weak, so this core locking phenomenon may be related to strong coupling between the 2/1 and 1/1 surfaces in ST geometry. The intrinsic error field may contribute to this coupling by limiting the differential rotation between the surfaces.

Both IPEC and M3D-C1 find the total resonant fields from the PF5 and OH errors are subdominant to that from the TF error. Error fields from eddy currents in the vacuum vessel and passive plates during IP ramp-up were also calculated using VALEN [15]. The resonant error fields from these currents were found to be below 1 G, and are therefore not presently considered to be a likely source of the observed error fields. The PF5 error field, while significant, is also expected to be more easily corrected by the NSTX-U RMP coils than the TF error field, especially when multiple response modes are important, due to the spectral similarity between the PF5 error field and RMP field.

Calculations of neoclassical toroidal viscosity done with GPEC [16] have been done for a number of NSTX-U model equilibria. Generally, higher NTV is found at higher β_N due to the increase in plasma response as marginal kink stability is approached [17]. In a typical case, GPEC found a total NTV torque on the order of 2 N-m in a high-beta NSTX-U model equilibrium. This compares with neutral beam torque of 1–2 N-m per source (depending strongly on the particular source), and is therefore not negligible. Unlike resonant fields, the NTV is a radially distributed torque that is quadratic in δB, and therefore cannot be completely compensated by external coils, even in the "single-mode" model. While NTV is an important consideration, setting coil tolerances based on NTV is challenging because the computed NTV torque strongly depends on the predicted rotation profile, which itself depends on torques from error fields. Due to this uncertainty, we believe that NTV calculations should not drive engineering tolerances.

Certain characteristics of the TF error field present new challenges for error field correction. Specifically, the error field spectrum differs significantly from that of coils on the low-field side (such as the NSTX-U RMP coils), and does not resonate strongly with the dominant kink mode, thus potentially requiring a multi-mode correction. Furthermore, IPEC calculations agree with experimental results in finding that that the optimal correction phase and amplitude changes as the plasma current density profile evolves, although the predicted correction phase disagrees with the empirical optimal phase after the formation of the q = 1 surface. This change in phase suggests that while EFC with the existing RMP coils may be possible, it would likely require a time-dependent correction algorithm that will be sensitive to plasma parameters (e.g. current density profile), and that is not easily predictable with present tools. This could pose a significant challenge to reliable operation of NSTX-U if the TF error is not reduced.

3.2. Divertor Heat Flux

Substantial heat loads on plasma facing components (PFCs) are predicted for high-performance NSTX-U scenarios. Mitigating surface heat flux through poloidal flux expansion may require BP /BT < 0.02. Error fields will lead to a toroidal variation in this pitch angle, and may therefore lead to toroidally localized regions of increased heat flux. Additionally, the formation of lobes due to the deformation of the topologically unstable x-point region in diverted plasmas can lead to an expansion of the wetted area of the divertor PFCs. This can have the beneficial effect of spreading the heat flux over a larger area, but it can also be problematic if it leads to toroidal localization of heat flux deposition or the deposition of heat outside of the intended target region.

To assess the impact of error fields on the magnetic footprint and pitch angle at the divertor plates, we have used the model NSTX-U equilibrium NSTX-U based on NSTX H-mode discharge 116313, with profiles scaled such that I_P = 2 MA and B_T = 1 T. Perturbed equilibria were calculated with M3D-C1, and the perturbation to the pitch angle was measured along the vertical and horizontal divertor plates (roughly R = 0.45 m and Z = −1.6 m, respectively. It is found that the maximum perturbation to the pitch angle due to the error field alone (in the absence of plasma response) at and is roughly 7.5 mrad (0.43°) and 1.5 mrad (.09°), respectively. The plasma response is generally found to increase the maximum perturbation to the pitch angle, especially at the horizontal target. The primary effect of the plasma response appears to be a toroidal phase shift of the perturbed field, with the maximum perturbed pitch angle remaining comparable to the vacuum field.

The divertor footprint was calculated using TRIP3D, taking the magnetic field from the M3D-C1 perturbed equilibrium calculations. Examples of these footprints for a 5 mm shift of the TF coil and the PF1A coil are shown in Fig. 3. For a given perturbation spectrum, we find that the linear extent of the footprint on the divertor scales linearly with the perturbation amplitude. Thus, to the extent that the plasma response remains linear in the error field strength, the footprint extent will depend linearly on the shift, tilt, and current in a coil.

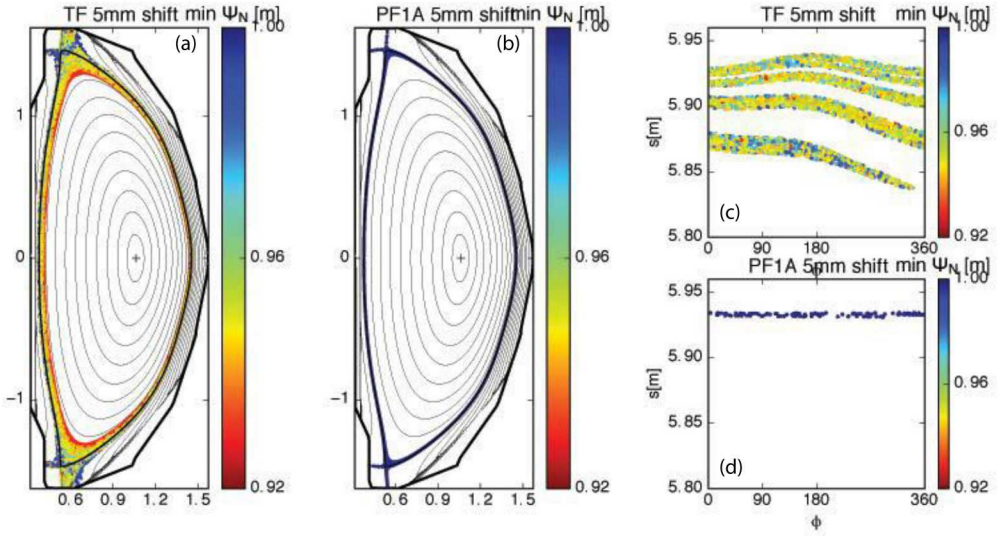

FIG 3. Poincare plot of the magnetic field lines that hit the wall due to a 5 mm shift of the TF center rod (a) and of the PF1AL (b). The footprints on the lower horizontal divertor from the two shifts are shown respectively in (c) and (d). The colors represent the minimum φ_N reached by each field line.

4. DISCUSSION

Experiments, metrology, and perturbed equilibrium modeling all suggest that the dominant source of field error in the 2016 NSTX-U configuration was likely from the misalignment of the TF rod. This field error is dominantly $m = n = 1$, which is not expected to strongly couple to the plasma through resonant interaction (i.e. excitation of kink modes). Indeed, calculations of the plasma response with IPEC and M3D-C1 both find relatively weak coupling of the TF error field to the plasma. Plasma response calculations from both codes suggest that the resonant currents elicited by the TF error field are comparable to those elicited by the RMP coils powered at 1 kA, despite the significantly larger vacuum fields from the TF error. IPEC modeling also found good agreement between the predicted and measured optimal error field correction in the early phase of an NSTX-U discharge, but poor agreement in the late phase, when the $q = 1$ surface was present. The failure to correct these error fields without causing a 1/1 locking event is clear evidence that multiple response modes are important. This, combined with the large change in the optimal error field correction phase during the discharge, present serious challenges for the correction of the error fields in NSTX-U as assembled in 2016.

To avoid these difficulties when NSTX-U resumes operations, we seek to use our understanding of the effect of error fields on the plasma to set physics-based tolerances for the alignment of magnets and plasma facing components (PFCs). Physics requirements on the 2/1 resonant field and magnetic pitch angles on PFCs independently limit the allowable misalignement of magnets and PFCs. The constraint that the vacuum or total 2/1 field is correctable by 1 kA-turn in the NSTX-U RMP coil limits the allowable tilt and shift of each coil to the values shown in Fig. 4, using data from M3D-C1 calculations of NSTX-U discharge 204077. The constraint that the perturbation to the magnetic pitch at the divertor targets is less than 10% yields the limits in Fig. 5, using data from M3D-C1 calculations of a NSTX-U model scenario 116313. The NSTX-U scenarios that we plot here are chosen because we believe them to yield conservative tolerances—204077 is a low-density, low-pressure case that couples relatively poorly to the RMP coils; and 116313 is a high-pressure, high flux expansion case with shallow equilibrium pitch angles. It is generally found that core locking considerations drive the tolerance requirements for the TF and vertical field coils (PF4s and PF5s), whereas magnetic pitch constraints drive the tolerances of the TF and divertor coils (PF1s, PF2s). Tolerances driven by core locking considerations refer to the relative alignment of magnets to each other, and tolerances driven by pitch angle considerations refer to the relative alignment of magnets and plasma facing components. It is also generally found that the calculation of pitch angle perturbations is relatively insensitive to the plasma response (with a probably spurious anomaly in the PF1A calculation) due to the relative distance of the response currents and the weak $n = 1$ coupling of the divertor coils to the plasma. These results, together with calculations for other NSTX-U equilibria and model scenarios, have been used to drive new engineering tolerance requirements for NSTX-U as it is rebuilt.

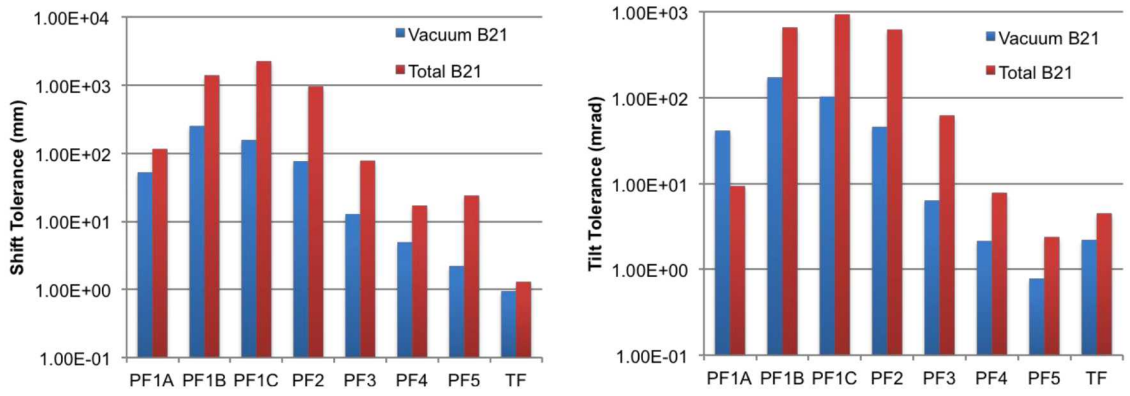

*FIG 4. Independent tolerances for the shift (*left*) and tilt (*right*) of various coils to reduce the 2/1 resonant vacuum field (*blue*) or total field (*red*) to less than that produced by 1 kA-turn in the NSTX-U RMP coils.*

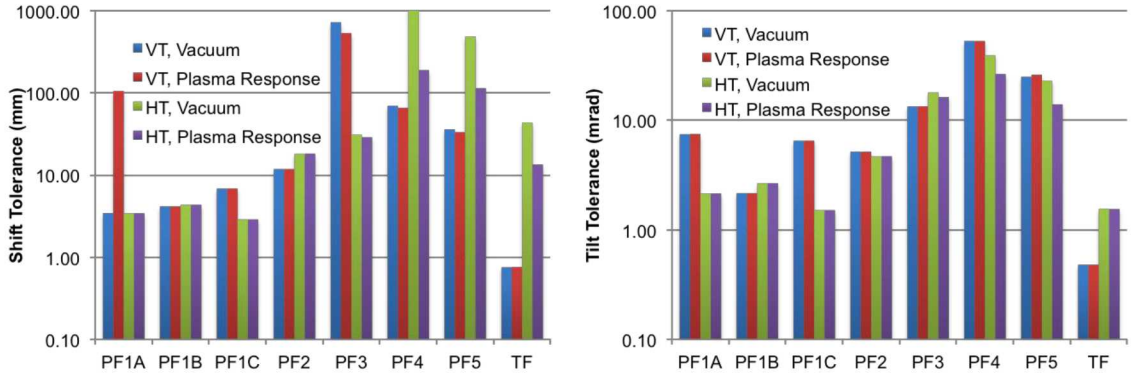

*FIG 5. Independent tolerances for the shift (*left*) and tilt (*right*) of NSTX-U coils to reduce the perturbed magnetic pitch angle at the divertor strike points on the vertical target (VT) and horizontal target (HT) to less than 10% of the equilibrium value. Tolerances are calculated using both the vacuum fields and total field.*

A trial fit-up of the TF center rod has found that it can be aligned to the CS casing to within 0.4 mm and 0.14 mrad. This should alleviate concerns about toroidally localized heating of the inner vessel plasma facing components, which are aligned to the CS casing. This should also simplify the reduction of magnetic braking and locking by providing a clear reference frame for aligning the vertical field coils. If this alignment can be made successfully, we expect a dramatic reduction in electromagnetic torque and an expansion of accessible parameter space (particularly with regard to density and collisionality) when NSTX-U resumes operation.

ACKNOWLEDGEMENTS

We thank J. Bialek for a VALEN calculation of the vessel currents during an NSTX-U current ramp. This work was supported by the U.S. Department of Energy under contract DE-AC02-09CH11466.

REFERENCES

[1] Fitzpatrick, R., Interaction of tearing modes with external structures in cylindrical geometry, *Nucl. Fusion* **33** (1993) 1049.

[2] Shaing, K.C., Magnetohydrodynamic-activity-induced toroidal momentum dissipation in collisionless regimes in tokamaks, *Phys. Plasmas* **10** (2003) 1443.

[3] Hender, T.C., *et al.*, Effect of resonant magnetic perturbations on COMPASS-C tokamak discharges, *Nucl. Fusion* **32** (1992) 2091.

[4] Evans, T.E., *et al.*, RMP ELM suppression in DIII-D plasmas with ITER similar shapes and collisionalities. Nucl. Fusion **48** (2008) 024002.

[5] Wolfe, S.M., *et al.*, Nonaxisymmetric field effects on Alcator C-Mod, *Phys. Plasmas* **12** (2005) 056110.

[6] Buttery R.J., *et al.*, Error field experiments in JET, *Nucl. Fusion* **40** (2000) 807.

[7] Menard, J.E., *et al.*, β-limiting MHD instabilities in improved-performance NSTX spherical torus plasmas, *Nucl. Fusion* **43** (2003) 330.

[8] Par, J.-K., *et al.*, Error field correction in ITER, *Nucl. Fusion* **48** (2008) 045006.

[9] Paz-Soldan, C., *et al*., The spectral basis of optimal error field correction on DIII-D, *Nucl. Fusion* **54** (2014) 073013.

[10] Menard, J.E., *et al*., Overview of NSTX Upgrade initial results and modelling highlights, *Nucl. Fusion* **57** (2017) 102006.

[11] La Haye, R.J., and Scoville, J.T., A method to measure poloidal field coil irregularities in toroidal plasma devices, *Rev. Sci. Instrum.* **62** (1991) 2146.

[12] Park, J.-K., Boozer, A.H., and Glasser, A.H., Computation of three-dimensional tokamak and spherical torus equilibria. *Phys. Plasmas* **14** (2007) 052110.

[13] Ferraro, N.M., Calculations of two-fluid linear response to non-axisymmetric fields in tokamaks. *Phys. Plasmas*, **19** (2012) 056105.

[14] Ferraro, N.M., *et al.*, Multi-region approach to free-boundary three-dimensional tokamak equilibria and resistive wall instabilities, *Phys. Plasmas* **23** (2016) 056114.

[15] Bialek, J., *et al.*, Modeling of active control of external magnetohydrodynamic instabilities, *Phys. Plasmas*, **8** (2001) 2170.

[16] Park, J.-K., and Logan, N.C., Self-consistent perturbed equilibrium with neoclassical toroidal torque in tokamaks, *Phys. Plasmas* **24** (2017) 032505.

[17] Boozer, A.H., Error field amplification and rotation damping in tokamak plasmas, *Phys. Rev. Lett.* **86** (2001) 5059.